Energy-Saving Control of Single-Rod Hydraulic Cylinders with Programmable Valves and Improved Working Mode Selection

Song Liu Bin Yao
School of Mechanical Engineering

Purdue University

West Lafayette, IN 47907, USA

ABSTRACT

This paper studies the energy-saving adaptive robust precision motion control of a single-rod hydraulic cylinder through the use of programmable valves. The programmable valves used in this study is a unique combination of five proportional cartridge valves connected in such a way that the meter-in and meter-out flows can be independently controlled by four of the valves as well as a true cross port flow controlled by the fifth valve. The programmable valves decouple the meter-in and meter-out flows providing tremendous flexibility to control the cylinder motion while decreasing the energy usage by utilizing the potential and kinetic energy of the load. This paper investigates the different working conditions of the programmable valves and proposes a simple yet effective way to use the programmable valves based on the desired states and current states.

INTRODUCTION

The use of hydraulic systems is widespread throughout industry due to the large power to size ratio. Hydraulic systems are used very heavily in the construction and agricultural industries and are well suited for these applications. In recent years, the trend is to replace the mechanical valve with an electrically controlled valve. The use of electro-hydraulic valves means that sophisticated electronic control can be applied to control the system.

The control of a hydraulic system is far from trivial, due to the highly nonlinear hydraulic dynamics [9]. In addition, parameters such as the bulk modulus change drastically with changing oil temperature and component wear. In the case of construction and agricultural machinery, the mechanical system driven by the hydraulic cylinder may be highly nonlinear itself. Typically, the parameters of the mechanical linkages may vary drastically and are usually unknown, such as the external payload. In addition, significant uncertain nonlinearities such as external disturbances, leakages and friction are unknown and cannot be modeled accurately [3]. These factors result in significant difficulties in controlling a hydraulic system.

The advent of electro-hydraulic valves and the incorporation of complex digital control have significantly improved the performance of hydraulic systems. A system using a conventional four-way directional control valve would be able to meet the high performance specification as shown by Bu and Yao [3], but would not be able to simultaneously provide precise motion control and individual cylinder chamber pressure control for better energy saving. With a typical four-way directional control valve only one of the two cylinder states, (pressures), is completely controllable and there is a one-dimensional internal dynamics. Although the one-dimensional internal dynamics is shown to be stable [3], it cannot be modified by any control strategy. The control input is uniquely determined once the desired motion is specified, which makes the regulation of individual cylinder chamber pressures impossible for energy-saving. The result is that while high performance tracking can be attained, simultaneous high levels of energy saving cannot. The uncontrollable state is due to the fact that the meter-in and meter-out orifices are mechanically linked together in a typical directional control valve. This is a fundamental drawback of typical four-way directional control valves. If this link were to be broken, the flexibility of the valve could be drastically increased, making the way for significant improvements in hydraulic efficiency [6].

The technique of breaking the mechanical linkage between the meter-in and meter-out orifices is well known and has been used in heavy industrial applications for several years. Typically, the spool valve is replaced by four poppet type valves [6]. There are a number of slight variations on this theme throughout the

mobile hydraulics industry. Patents by Deere & Company, Moline, IL as well as Caterpillar Inc., Joliet, IL. and Moog Inc., East Aurora, NY attest to the potential of this technique [7,1,5]

The valve configuration used in this study takes the four-valve poppet type valve and makes the addition of an additional valve to enable true cross port flow. The configuration allows independent meter-in, meter-out control in addition to the availability of cross port regenerative flow. The result is a programmable valve capable of controlling each cylinder state as well as providing regeneration flow for optimal energy usage. The programmable valve configuration used in this study is seen in Figure 1.

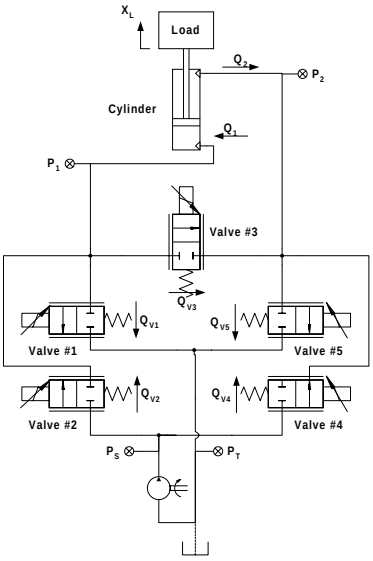

Figure 1. Programmable Valve Layout

The use of the programmable valve provides multiple inputs to control the two cylinder states. The effect is that both cylinder states, P_1 and P_2, become completely controllable. In fact, there are multiple ways of controlling both cylinder states, which makes the objectives of having both precise motion control and energy-savings possible.

The objective of this study is to investigate the simple and yet effective use of the programmable valve in achieving the dual objectives of high performance motion tracking and high energy saving. Different from previous works, this paper presents a working mode selection method based on the desired states and trajectory as well as the current pressures. The programmable valve is implemented on a robot arm modeled after an industrial backhoe emulating a typical hydraulic system.

The specific controller structure is composed of a task level controller and a valve level controller. The task level controller calculates the desired cylinder force and determines the working mode of programmable valve. The valve level controller includes a pressure regulator algorithm to maintain low off-side chamber pressures and an adaptive robust controller to provide effective motion control in spite of the various uncertainties and nonlinearities.

The rest of the paper is organized as: section 1 introduces the experiment setup and dynamic model. The desired cylinder force based working mode selection is detailed in Section 2. Section 3 provides the off-side pressure regulator and working side ARC motion controller. Section 4 shows the simulation and experiment results and Section 5 concludes the paper.

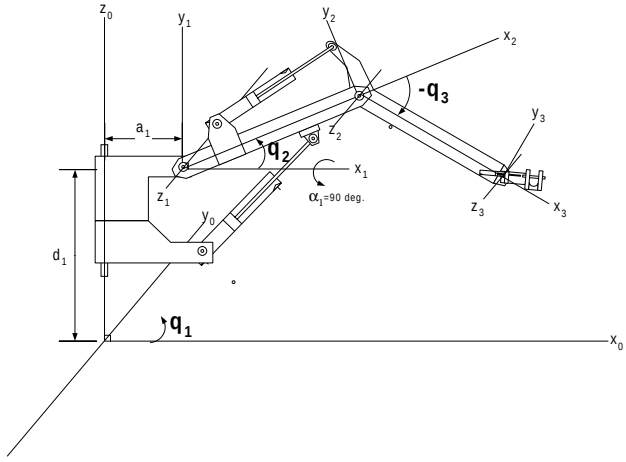

Figure 2. Coordinate System of the Hydraulic Robot Arm

1 PROBLEM FORMULATION AND DYNAMIC MODEL

This paper focuses on the boom motion control of a three degree-of-freedom electro-hydraulic robot arm. The coordinate systems, joint angles and physical parameters of the system are defined as in Fig. 2. The dynamic equations describing the electro-hydraulic robot arm are taken directly from Bu and Yao [4]. The dynamics of the boom motion can be described by

$$\begin{aligned}(J_c + m_L l_e^{\,2})\ddot{q}_2 + G_c(q_2) + m_L g l_g(q_2) \\ = \frac{\partial x_L}{\partial q_2}(P_1 A_1 - P_2 A_2) + T(t, q_2, \dot{q}_2)\end{aligned} \quad (1)$$

where P_1 and P_2 are the head and rod end pressures of the cylinder respectively, A_1 and A_2 are the head and rod end areas of the cylinder respectively, $T(t, q_2, \dot{q}_2)$ represents the lumped disturbance torque including external disturbances and terms like the friction torque. In (1), the terms J_c, $G_c(q_2)$, $l_g(q_2)$ and $l_e^{\,2}$ are defined as:

$$
\begin{aligned}
J_c &= I_2 + 2m_2 l_2 x_b + m_2 l_2^{\,2} + I_3 + m_3(l_2^{\,2} + l_3^{\,2} + 2l_2 l_3 c_3) \\
&\quad + 2m_3 l_2 x_{st} c_3 - 2m_3 l_2 y_{st} s_3 \\
G_c(q_2) &= m_2 g l_2 c_2 + m_2 g x_b c_2 - m_2 g y_b s_2 + m_3 g(l_2 c_2 + l_3 c_{23}) \\
&\quad + m_3 g(x_{st} c_{23} - y_{st} s_{23}) \\
l_g(q_2) &= l_2 c_2 + l_3 c_{23} \\
l_e^{\,2} &= l_2^{\,2} + l_3^{\,2} + 2l_2 l_3 c_3
\end{aligned}
\tag{2}
$$

where x_b and y_b are the coordinates of the boom center of gravity with respect to the $x_2 y_2 z_2$ coordinate frame, x_{st} and y_{st} are the coordinates of the stick center of gravity with respect to the $x_3 y_3 z_3$ coordinate frame, I_2 is the moment of inertia of the boom arm about the z_2 axis, I_3 is the moment of inertia of the stick arm about the z_3 axis, c_2, s_2, c_3, s_3, c_{23}, s_{23} are shorthand notations for $\cos(q_2)$, $\sin(q_2)$, $\cos(q_3)$, $\sin(q_3)$, $\cos(q_2+q_3)$ and $\sin(q_2+q_3)$ respectively, m_2 is the mass of the boom arm, m_3 is the mass of the stick arm and m_L is the unknown mass of the inertial loaded attached to the end of the stick arm. The inertial load is assumed to be a point mass for the sake of simplicity.

The inertial moment and the gravity force both depend on the unknown element m_L. As a result, the inertial moment and the gravity force are split into two components. The terms J_c and $G_c(q_2)$ contain only calculable quantities and the terms $m_L g l_g(q_2)$ and $m_L l_e^{\,2}$ which contain the unknown quantity m_L. The unknown terms have to be estimated later on-line via parameter adaptation.

Neglecting cylinder leakage, the cylinder equations can be written as [9],

$$
\begin{aligned}
\frac{V_1(x_L)}{\beta_e}\dot{P}_1 &= -A_1\dot{x}_L + Q_1 = -A_1\frac{\partial x_L}{\partial q_2}\dot{q}_2 + Q_1 \\
\frac{V_2(x_L)}{\beta_e}\dot{P}_2 &= A_2\dot{x}_L - Q_2 = -A_2\frac{\partial x_L}{\partial q_2}\dot{q}_2 - Q_2
\end{aligned}
\tag{3}
$$

where $V_1(x_L) = V_{h1} + A_1 x_L$ and $V_2(x_L) = V_{h2} - A_2 x_L$ are the total cylinder volumes of the head and rod end respectively, V_{h1} and V_{h2} are the initial control volumes when $x_L = 0$, β_e is the effective bulk modulus. Q_1 and Q_2 are the supply and return flows respectively.

For the programmable valve in Fig. 1, Q_1 and Q_2 are given by,

$$
\begin{aligned}
Q_1 &= Q_{v2} - Q_{v1} - Q_{v3} \\
Q_2 &= Q_{v5} - Q_{v4} - Q_{v3}
\end{aligned}
\tag{4}
$$

where the orifice flows Q_{vi} can be described by

$$
\begin{aligned}
Q_{v1} &= f_{v1}(\Delta P_{v1}, x_{v1}) \qquad \Delta P_{v1} = P_1 - P_t \\
Q_{v2} &= f_{v2}(\Delta P_{v2}, x_{v2}) \qquad \Delta P_{v2} = P_s - P_1 \\
Q_{v3} &= f_{v3}(\Delta P_{v3}, x_{v3}) \qquad \Delta P_{v3} = P_1 - P_2 \\
Q_{v4} &= f_{v4}(\Delta P_{v4}, x_{v4}) \qquad \Delta P_{v4} = P_s - P_2 \\
Q_{v5} &= f_{v5}(\Delta P_{v5}, x_{v5}) \qquad \Delta P_{v5} = P_2 - P_t
\end{aligned}
\tag{5}
$$

in which f_{vi} is the nonlinear orifice flow mapping as a function of the pressure drop, ΔP_{vi} and the orifice opening, x_{vi}, of the *ith* cartridge valve. x_{vi} is related to the command voltage by the transfer function equation (6).

$$
\frac{x_{vi}(s)}{v_i(s)} = \frac{\omega_v^2}{s^2 + 2\xi_v\omega_v s + \omega_v^2}
\tag{6}
$$

where the natural frequency and the damping ration are $\omega_v = 353.6 rad/\sec$ and ξ_v=1.03 respectively.

Due to the fact that the nonlinear flow mappings are very difficult to determine accurately, it is assumed that

$$
\begin{aligned}
Q_1 &= Q_{1M} + \tilde{Q}_1 \\
Q_2 &= Q_{2M} + \tilde{Q}_2
\end{aligned}
\tag{7}
$$

where Q_{1M} and Q_{2M} represent the flows from the approximated valve mappings and $\tilde{Q}_1$ and $\tilde{Q}_2$ represent the modeling errors of the flow mappings. The effect of the errors will be dealt with through robust feedback.

In this adaptive robust controller design the parametric uncertainties due to the unknown payload m_L, the bulk modulus β_e, the nominal value of the lumped disturbance T, T_n are considered as parameters to be adapted. In order to use parameter adaptation to reduce parametric uncertainties to improve performance, it is necessary to linearly parameterize the system dynamics equation in terms of a set of unknown parameters. To achieve this, define the unknown parameter set $\theta = [\theta_1, \theta_2, \theta_3]^T$ as $\theta_1 = \dfrac{1}{1 + \dfrac{l_e^{\,2}}{J_c} m_L}$, $\theta_2 = \dfrac{T_n}{J_c + m_L l_e^{\,2}}$, $\theta_3 = \beta_e$ The system dynamics equation can thus be linearly parameterized in terms of θ as

$$
\begin{aligned}
\ddot{q}_2 &= \frac{\theta_1}{J_c}[\frac{\partial x_L}{\partial q_2}(P_1 A_1 - P_2 A_2) - G_c(q_2)] + \frac{\theta_1}{l_e^{\,2}} g l_g - \frac{1}{l_e^2} g l_g \\
&\quad + \theta_2 + \tilde{T}(t, q_2, \dot{q}_2) \\
\dot{P}_1 &= \frac{\theta_3}{V_1(q_2)}(-A_1\frac{\partial x_L}{\partial q_2}\dot{q}_2 + Q_{1M} + \tilde{Q}_{1M}) \\
\dot{P}_2 &= \frac{\theta_3}{V_2(q_2)}(A_2\frac{\partial x_L}{\partial q_2}\dot{q}_2 - Q_{2M} + \tilde{Q}_{2M})
\end{aligned}
\tag{8}
$$

where $\tilde{T} = \dfrac{T(t,q_2,\dot{q}_2) - T_n}{J_c + m_L l_e^2}$ and the unknown parameters θ_1, θ_2, θ_3 and uncertain nonlinearities, $\tilde{T}$, are physically bounded. Furthermore it is assumed that

$$\begin{aligned} \left|\tilde{Q}_{1M}(x_v,\Delta P_1)\right| &\le \delta_{Q1}(\Delta P_1) \\ \left|\tilde{Q}_{2M}(x_v,\Delta P_2)\right| &\le \delta_{Q2}(\Delta P_2) \end{aligned} \tag{9}$$

where $\delta_{Q1}(\Delta P_1)$ and $\delta_{Q2}(\Delta P_2)$ are known.

Given the desired motion trajectory $q_{2Ld}(t)$, the first objective is to synthesize valve control voltages such that the output $y = q_2$, tracks $q_{2Ld}(t)$ as closely as possible in spite of various model uncertainties. The second objective is to minimize the overall energy loss.

2 WORKING MODE SELECTION

The proposed working mode selection is different from precious work in that the previous working mode selection is based on the current cylinder velocity and cylinder force, but the proposed method uses the desired cylinder force and velocity, as well as the current pressure at the two chambers. So the first step of mode selection is the calculation of desired cylinder force.

The calculation of desired cylinder force is taken from the ARC controller design in Bu and Yao's work [3,4]. Define a switching-function-like quantity as

$$\begin{aligned} z_2 &= \dot{z}_1 + k_1 z_1 = \dot{q}_2 - \dot{q}_{2r}, \\ \dot{q}_{2r} &= \dot{q}_{2d} - k_1 z_1 \end{aligned} \tag{10}$$

where $z_1 = q_2(t) - q_{2d}(t)$, $q_{2d}(t)$ is the desired trajectory and k_1 is any positive feedback gain. The design in this step is to make z_2 as small as possible with a guaranteed transient performance. To this end, differentiating (10) and noting (8)

$$\begin{aligned} \dot{z}_2 = \ddot{q}_2 - \ddot{q}_{2r} &= \frac{\theta_1}{J_c}\left[\frac{\partial x_L}{\partial q_2}(P_1A_1 - P_2A_2) - G_c(q_2)\right] \\ &+ \frac{1}{l_e^2}\theta_1 g l_g(q_2) - \frac{1}{l_e^2} g l_g + \theta_2 + \tilde{T} - \ddot{q}_{2r} \end{aligned} \tag{11}$$

where $\ddot{q}_{2r} = \ddot{q}_{2d} - k_1\dot{z}_1$ is calculable. In (11), define the load force as $P_L = P_1A_1 - P_2A_2$. If we treat P_L as the virtual control input to (11), we can synthesize a virtual control law P_{Ld} for P_L such that z_2 is as small as possible. Since (11) have both parametric uncertainties θ_1 and θ_2 and uncertain nonlinearity $\tilde{T}$, the ARC approach proposed by Yao [10] will be generalized to accomplish the objective.

The control function P_{Ld} consists of two parts give by

$$\begin{aligned} P_{Ld}(q_2,\dot{q}_2,\hat{\theta}_1,\hat{\theta}_2,t) &= P_{Lda} + P_{Lds} \\ P_{Lda} &= \frac{\partial q_2}{\partial x_L}\left[G_c(q_2) + \frac{J_c}{\hat{\theta}_1}\left(-\frac{\hat{\theta}_1}{l_e^2} g l_g + \frac{1}{l_e^2} g l_g - \hat{\theta}_2 + \ddot{q}_{2r}\right)\right] \end{aligned} \tag{12}$$

in which P_{Lda} functions as an adaptive control law used to achieve an improved model compensation through on-line parameter adaptation as defined by Bu and Yao [4], and P_{Lds} is a robust control law to be synthesized later. If P_L were the actual control input, then τ as defined by Bu and Yao [4] would be

$$\begin{aligned} \tau_2 &= \omega_2 \phi_2 z_2 \\ \phi_2 &= \left[\frac{1}{J_c}\left(\frac{\partial x_L}{\partial q_2} P_{Lda} - G_c\right) + \frac{1}{l_e^2} g l_g, 1, 0\right]^T \end{aligned} \tag{13}$$

where ω_2>0 is a constant weighting factor. Due to the use of discontinuous projection, the adaptation law as given by Bu and Yao [4] is discontinuous and thus cannot be used in the control law design at each step as contrary to the tuning function based backstepping adaptive control [8]. Backstepping design needs the control function synthesized at each step to be sufficiently smooth in order to obtain its partial derivatives. To compensate for this loss of information, the robust control law has to be strengthened. So the robust control function P_{Lds} consists of two terms given by

$$\begin{aligned} P_{Lds} &= P_{Lds1} + P_{Lds2} \\ P_{Lds1} &= -\frac{J_c}{\theta_{1\min}}\frac{\partial q_2}{\partial x_L} k_2 z_2 \end{aligned} \tag{14}$$

where k_2 is a positive feedback gain. P_{Lds1} is a proportional feedback term with a time-varying nonlinear gain, and P_{Lds2} is a robust control function synthesized as follows. Let $z_3 = P_L - P_{Ld}$ denote the input discrepancy. Substituting (12) and (14) into (11) while noting (13),

$$\begin{aligned} \dot{z}_2 &= \frac{\theta_1}{J_c}\frac{\partial x_L}{\partial q_2} z_3 - \frac{\theta_1}{\theta_{1\min}}(k_2 + k_{2s1}) z_2 \\ &+ \frac{\theta_1}{J_c}\frac{\partial x_L}{\partial q_2} P_{Lds2} - \tilde{\theta}^T \phi_2 + \tilde{T} \end{aligned} \tag{15}$$

The robust control function P_{Lds2} is now chosen to satisfy the following conditions

$$\begin{aligned} &i && z_2\left[\frac{\theta_1}{J_c}\frac{\partial x_L}{\partial q_2} P_{Lds2} - \tilde{\theta}^T \phi_2 + \tilde{T}\right] \le \varepsilon_2 \\ &ii && z_2 \frac{\partial x_L}{\partial q_2} P_{Lds2} \le 0 \end{aligned} \tag{16}$$

where ε_2 is a design parameter which can be arbitrarily small. Essentially, condition i of (16) shows that P_{Lds2} is synthesized to dominate the model uncertainties coming from both parametric uncertainties $\tilde{\theta}$ and uncertain nonlinearities $\tilde{T}$, and condition ii is to make sure that P_{Lds2} is dissipating in nature so that it does not interfere with the functionality of the adaptive control part P_{Lda}. How to choose P_{Lds2} to satisfy constraints like (16) can be found in the work done by Yao and Tomizuka [11,12].

Because the robust control function P_{Lds} is chosen to dominate the disturbances and uncertainties and depends on feedback tracking error, it is sensitive to noise and changes quickly, which may cause high frequency mode switching. To keep the cylinder working at relatively stable manner, only P_{Lda} is used for the working mode selection.

The utilization of the programmable valve is decided by different working conditions, which is shown in Table1. According to the desired velocity $\dot{x}_d$ and force P_{Lda}, five tracking modes Ti (i=1…5) and two regulating modes, Ri (i=1,2), are defined.

Table 1. Programmable valve working conditions

$\dot{x}_d$	P_{Lda}	Valve Configuration	Off-side	Mode
>0	>0	$Q_1 = Q_{v2}$ $Q_2 = Q_{v5}$	P2	T1
	<0	$Q_1 = Q_{v2} - Q_{v3}$ $Q_2 = Q_{v3}$	P1	T2
<0	>0 $(P_1 > P_2)$	$Q_1 = -Q_{v3}$ $Q_2 = -Q_{v3} + Q_{v5}$	P2	T3
	>0 $(P_1 \le P_2)$	$Q_1 = -Q_{v1}$ $Q_2 = -Q_4$	P2	T4
	<0	$Q_1 = -Q_{v1}$ $Q_2 = -Q_{v4}$	P1	T5
=0	>0	$Q_1 = Q_{v2}$ $Q_2 = Q_{v5}$	P2	R1
	<0	$Q_1 = -Q_{v1}$ $Q_2 = -Q_{v4}$	P1	R2

Mode T1 represents a standard working conditions, in which the control command calls for the cylinder to be extended with a resistive load. The most efficient usage of the programmable valves is to use valve 2 to provide the control flow Q_1 for the head end chamber and to use the valve 5 to maintain a low pressure in the rod end chamber.

In mode T2, the cylinder may extend under an external overrunning force or in a deceleration period, and $P_2 > P_1$, which enables the regeneration flow from rod end chamber to head end chamber. This reduces the flow needed from the pump and energy usage dramatically. Flow from the pump is still needed due to the large head end area. In this case, valve 3 is used to control the cylinder motion and valve 2 is used to maintain the desired low pressure in head end chamber.

Mode T5 is another standard operation in that the cylinder is to be retraced under a resistive load. Valve 4 is used to provide the control flow while valve 1 is used to maintain the head end pressure at low level.

Mode T4 is used in the situation that the cylinder is to be retracted under an overrunning external force or in a deceleration period, but the head end pressure P_1 is not higher than the rod end pressure P_2. In this mode, valve 1 is used to control the cylinder motion and valve4 is used to regulate the rod end pressure to the desired low level.

Mode T3 occurs under the similar condition as T4, with the additional constraint that $P_1 > P_2$, which ensures that the regeneration flow can be pumped from the head end chamber to the rod end chamber through valve 3. The excess flow due the large head end area is drained to the tank though valve 5. In this mode, valve 3 is used to control cylinder motion while valve 5 to regulate the desired low pressure at rob end chamber. This results an operation requiring no pump flow.

When the desired velocity is zero, the cylinder is working in a position regulating mode. In this mode, the movement of the cylinder rod is usually very small and the velocity may switch rapidly to maintain smallest position error. No regeneration flow is expected to use in this mode. Regulation mode R1 works same as mode T1 while R2 as T5.

3 CONTROLLER DESIGN

The primary goal in the development of a controller for the electro-hydraulic robot arm is precise motion control. The secondary objective of the design is to minimize energy loss and optimize the energy usage of the system. In order to minimize energy loss of the system, the pressures of the cylinder must be kept to the minimum needed for precise motion control.

In order to achieve these very significant gains a controller must be developed that can handle the task of precise motion control and simultaneous pressure control. In addition, the design is complicated by the highly nonlinear nature of the system, large variation in parametric uncertainties, large external disturbances, unmodeled friction forces, mismatched model uncertainties, nonlinear flow behavior of the valves and

the difficulty of coordinated control of five independent valves.

The solution to this complex problem is the use of a nonlinear model based adaptive robust controller to directly deal with the nonlinear system, uncertain parameters, uncertain nonlinearities and mismatched model uncertainties to provide the desired load flow that is needed for precise motion control. The controller is composed of two independent parts: off-side pressure regulator and working side motion controller. The off-side pressure regulator, which consists of model compensation and robust feedback, is used to handle the pressure regulation of the off-side chamber for optimizing energy usage. The ARC approach proposed by Yao [10] will be generalized to accomplish the objective of precision motion control.

Off-side Pressure Regulator Design

The pressure controller design is intended to regulate the pressure of the off-side of the cylinder. The working side is defined as the side critical to the motion of the cylinder and the off-side is defined as the other end where cylinder pressure can be arbitrarily set. The working and off-sides of the cylinder change depending on the working conditions of the robot arm. As the off-side cylinder flow changes, the working side flow must be adjusted as well to maintain the desired cylinder flow critical to precise motion control. First it must be determined how to control the pressure in one side of the cylinder. The cylinder dynamics are described by (3) and (7). In order to use parameter adaptation to reduce parametric uncertainties to improve performance, it is necessary to linearly parameterize the system dynamics in terms of a set of unknown parameters θ_p. θ_p is defined as $\theta_p = [\theta_\beta, \theta_Q]^T$, where $\theta_\beta = 1/\beta_e$, θ_Q is the nominal value of $\tilde{Q}_1$, i.e. $\tilde{Q}_1 = \theta_Q + \Delta Q_1$. The cylinder dynamics for the head end chamber can be rewritten as follows.

$$\dot{P}_1 = \frac{1}{\theta_\beta V_1}(-A_1 \dot{x}_L + Q_{1M} + \theta_Q + \Delta Q_1) \tag{17}$$

Assume $|\theta_Q| = |\tilde{Q}_1| \le \delta_{Q1}$ and $|\theta_\beta| \le \delta_\beta$, δ_{Q1} and δ_β are know functions. The goal is to have the cylinder pressure regulated to a desired pressure. For the head end pressure P_1, this is written as

$$e_{P1} = P_1 - P_{1d} \tag{18}$$

where ep_1 is the difference between the actual pressure and the desired one and P_{1d} is the desired head end pressure. Taking the derivative of (18), we obtain

$$\dot{e}_{p1} = \dot{P}_1 - \dot{P}_{1d} = \frac{1}{\theta_\beta V_1}(-A_1 \dot{x}_L + Q_{1M} + \theta_Q + \Delta Q_1) - \dot{P}_{1d} \tag{19}$$

Q_{1M} is the control input and the control law can be defined as

$$\begin{aligned} Q_{1M} &= Q_{1Ma} + Q_{1Ms} \\ Q_{1Ma} &= A_1 \dot{x}_L + \hat{\theta}_\beta V_1 \dot{P}_{1d} - \hat{\theta}_Q \\ Q_{1Ms} &= -k_p e_{p1} + Q_{1Ms2} \end{aligned} \tag{20}$$

Where Q_{1Ma} is a model compensation term, and Q_{1Ms} is a robust feedback term, Q_{1Ms2} is chosen such that the following conditions are satisfied:

$$\begin{aligned} e_{p1}\left[\frac{1}{V_1}(Q_{1Ms2} - \tilde{\theta}_Q - \Delta Q_1) - \theta_\beta \dot{P}_{1d}\right] &\le \varepsilon_p \\ e_{p1} Q_{1Ms2} &\le 0 \end{aligned} \tag{21}$$

where $\tilde{\theta}_Q = \hat{\theta}_Q - \theta_Q$, $\tilde{\theta}_\beta = \hat{\theta}_\beta - \theta_\beta$ and ε_p is a design parameter.

The adaptation law is then defined as:

$$\begin{aligned} \dot{\hat{\theta}}_\beta &= \mathrm{Pr}oj_{\theta_\beta}(-\gamma_\beta \dot{P}_{1d} e_{p1}) \\ \dot{\hat{\theta}}_Q &= \mathrm{Pr}oj_{\theta_Q}(\gamma_Q e_{p1}) \end{aligned} \tag{22}$$

The given adaptive robust adaptive robust control law (20), (21) and adaptation law (22) provides prescribed transient response in general and asymptotic tracking in the absence of uncertain disturbance. Theoretical proof can be seen in Appendix A.

The above controller is used in the case that the head end pressure is to be regulated. In the event that the rod end pressure is to be regulated, the controller can be designed similarly.

Working-side ARC Motion Controller Design

The working side ARC motion controller design would follow the desired cylinder force calculation in section 2.1 where we have already designed a virtual control input for pressure P_L, P_{Ld}, and defined the discrepancy $z_3 = P_L - P_{Ld}$. In this step, an actual control law for the state dynamics (8) will be synthesized so that z_3 converges to zero or a small value with a guaranteed transient performance and accuracy. The specific control law varies slightly depending on the different working modes. It is assumed that the pressure controller is able to maintain the off-side chamber pressure at the desired pressure, and the desired off-side pressure is used in this motion controller design, regardless of the actual chamber pressure.

The control design for that head end chamber is the working side is illustrated in this section, and the control design for that the rod end is the working side can be done in a similar way.

From (8)

$$\begin{aligned}\dot{z}_3 &= \dot{P}_L - \dot{P}_{Ld} \\ &= \theta_3\left[\frac{A_1^2}{V_1}\frac{\partial x_L}{\partial q_2}\dot{q}_2 + \frac{A_1}{V_1}Q_{1M} + \frac{A_1}{V_1}\tilde{Q}_1\right] - \dot{P}_{Ldc} - \dot{P}_{Ldu}\end{aligned} \quad (23)$$

where

$$\begin{aligned}\dot{P}_{Ldc} &= \frac{\partial P_{Ld}}{\partial q_2}\dot{q}_2 + \frac{\partial P_{Ld}}{\partial \dot{q}_2}\hat{\ddot{q}} + \frac{\partial P_{Ld}}{\partial t} \\ \dot{P}_{Ldu} &= \frac{\partial P_{Ld}}{\partial \dot{q}_2}\left[-\frac{1}{J_c}\left(\frac{\partial x_L}{\partial q_2}P_L - Gc\tilde{\theta}_1 - \frac{1}{l_e^2}gl_g\tilde{\theta}_1 - \tilde{\theta}_2 + \tilde{T}\right)\right] + \frac{\partial P_{Ld}}{\partial \hat{\theta}}\dot{\hat{\theta}} \\ \hat{\ddot{q}}_2 &= \frac{\hat{\theta}_1}{J_c}\left[\frac{\partial x_L}{\partial q_2}(P_1A_1 - P_2A_2) - G_c\right] + \frac{\hat{\theta}_1}{l_e^2}gl_g - \frac{1}{l_e^2}gl_g + \hat{\theta}_2\end{aligned} \quad (24)$$

In (24), $\hat{\ddot{q}}_2$ represent the calculable part of $\ddot{q}_2$, $\dot{P}_{Ldc}$ is calculable and can be used in the construction of control functions, but $\dot{P}_{Ldu}$ has to be dealt with via certain robust feedback in the motion controller design. Define the Q_{1L} and $\tilde{Q}_{1L}$ as

$$\begin{aligned}Q_{1L} &= \frac{A_1}{V_1}Q_{1M} \\ \tilde{Q}_{1L} &= \frac{A_1}{V_1}\tilde{Q}_1\end{aligned} \quad (25)$$

Then, in viewing (23), Q_{1L} can be thought as the virtual control input for (23) and this step is to synthesize a control function $\tilde{Q}_{1L}$ for Q_{1L} such that P_L tracks the desired control function P_{Ld} synthesized in section 2.1 with a guaranteed transient performance.

Define Q_{1Lde} and ϕ_3 as

$$\begin{aligned}Q_{1Lde} &= \frac{1}{J_c}\frac{\omega_2}{\omega_3}\frac{\partial x_L}{\partial q_2}z_2\hat{\theta}_1 - \frac{A_1^2}{V_1}\frac{\partial x_L}{\partial q_2}\dot{q}_2\hat{\theta}_3 - \dot{P}_{Ldc} \\ \phi_3 &= \begin{bmatrix} \dfrac{\omega_2}{\omega_3 J_c}\dfrac{\partial x_L}{\partial q_2}z_2 - \dfrac{\partial P_{Ld}}{\partial \dot{q}_2}\left[\dfrac{1}{J_c}\left(\dfrac{\partial x_L}{\partial q_2}P_L - G_c\right) + \dfrac{1}{l_e^2}gl_g\right] \\ -\dfrac{\partial P_{Ld}}{\partial \dot{q}_2} \\ -\dfrac{A_1^2}{V_1}\dfrac{\partial x_L}{\partial q_2}\dot{q}_2 + Q_{1Lda} \end{bmatrix} \\ \tau_3 &= \omega_3\phi_3 z_3\end{aligned} \quad (26)$$

Then the control law for Q_{1Ld} is designed as follows:

$$\begin{aligned}Q_{1Ld}(q_2, \dot{q}_2, P_1, P_2, \hat{\theta}, t) &= Q_{1Lda} + Q_{1Lds1} + Q_{1Lds2} \\ Q_{1Lda} &= -\frac{1}{\hat{\theta}_3}Q_{1Lde} \\ Q_{1Lds1} &= -\frac{1}{\theta_{3\min}}k_3 z_3\end{aligned} \quad (27)$$

where k_3 is a positive feedback gain, and Q_{1Lds2} is a robust control function satisfying the following two conditions:

$$\begin{aligned}z_3\left[\theta_3 Q_{1Lds2} + \theta_3\tilde{Q}_{1L} - \tilde{\theta}^T\phi_3 - \frac{\partial P_{Ld}}{\partial \dot{q}_2}\tilde{T} - \frac{\partial P_{Ld}}{\partial \hat{\theta}}\dot{\hat{\theta}}\right] &\le \varepsilon_3 \\ z_3 Q_{1Lds2} &\le 0\end{aligned} \quad (28)$$

where ε_3 is a design parameter.

The adaptation law is given by

$$\dot{\hat{\theta}} = \Pr oj_\theta(\Gamma\tau) \quad (29)$$

where $\tau = \tau_2 + \tau_3$ and Γ is the adaptation rate.

The ARC motion controller given by (12) (14) (16), (26), (27), (28) and adaptation law (29) can provide prescribed transient performance in general and asymptotic tracking in the absence of uncertain disturbance.

Once the control functions for working side and off-side are synthesized, the next step is to distribute the desired flow to the programmable valve according to the working mode selected. The last component of the programmable valve control system is to deal with the nonlinear valve flow via the nonlinear pressure compensated inverse valve mappings. The desired flows for each of the five programmable valves and the corresponding pressure drops for each valve are used as inputs to the inverse valve mapping and a lookup table determines the voltage input need for the given conditions. The effect is that the nonlinearities of the valves have been compensated for and the controller is now complete.

SIMULATION AND EXPERIMENTAL RESULTS

The completed controller is simulated in Simulink. The ARC motion controller parameters used in the simulations are: $k_1 = k_2 = k_3 = 55$, Γ=*diag (1e-12, 1e-10, 5e4)*. The parameters for the pressure regulators are $k_{p1} = 5.0\times10^{-10}$, $\gamma_{Q1} = 4.0\times10^{-8}$ $k_{p2} = 5.6\times10^{-10}$, $\gamma_{Q2} = 3.15\times10^{-8}$. The desired pressure is chosen to be constant, so $\dot{P}_{1d} = 0$, there is no adaptation for θ_β. The controller is simulated for two trajectories. A simple extend, stop, retract and stop point to point trajectory is used with and without a 50 pound external loading. A similar trajectory is also simulated with a larger step and

faster allowable velocity. The two input commands are shown in Fig. 3. The simulation results for the slow point to point trajectory with and without a 50 lb. load, Fig. 4 and Fig. 5, show that the controller performs very well in each case with a maximum error less than 0.01 *rad*. The cylinder pressures in both cases remain very low, thus increasing efficiency of the system. The energy usage is calculated as the pump flow times the pressure drop from pump to tank. The energy usage is zero when the cylinder is working in mode T3, as seen between the time of 5-9 seconds. The plot of the energy usage includes an additional line representing the potential decrease in energy usage with a load sensing pump. The current set up and simulation makes use of a constant pressure supply that is not highly efficient. A load sensing pump that can provide the needed flow at the highest working pressure would significantly reduce the energy usage if used in conjunction with the programmable valve. The plot labeled as 'LS Energy Usage' calculates the anticipated energy usage if a load sensing pump was used. It also assumes that the pump would track the highest working pressure and add an additional 500 KPa margin of pressure.

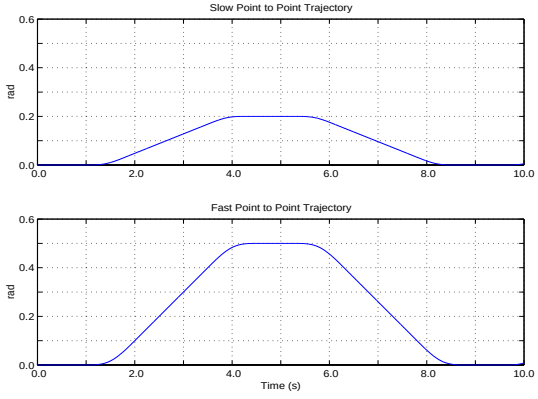

Figure 3. Point to Point Trajectories

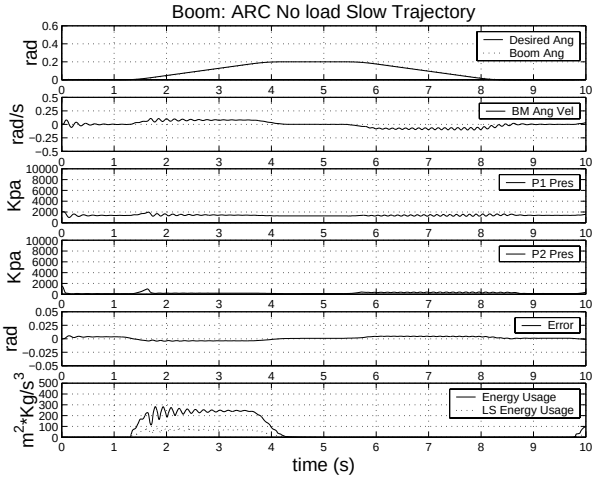

Figure 4. Boom ARC Sim: Slow Traj. No Load

Figs. 6 and 7 show similar simulations using a conventional servo valve and similar adaptive robust controller. These results are shown for the sake of comparison with the current results. While the tracking performance may be similar, significant improvements in terms of pump energy usage can be seen with the programmable valve. The cylinder pressures are significantly higher with the conventional valve and consequently the energy usage is larger. The same can be said if a load sensing pump is used in each case. The remainder of the simulation results can be seen in appendix C.

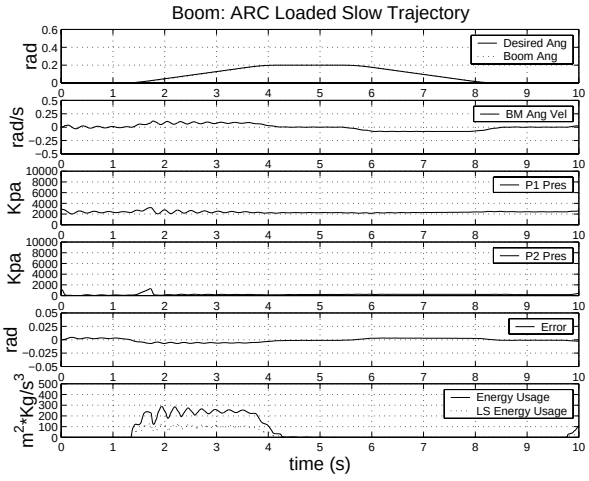

Figure 5. Boom ARC Sim: Slow Traj. 50lb. Load

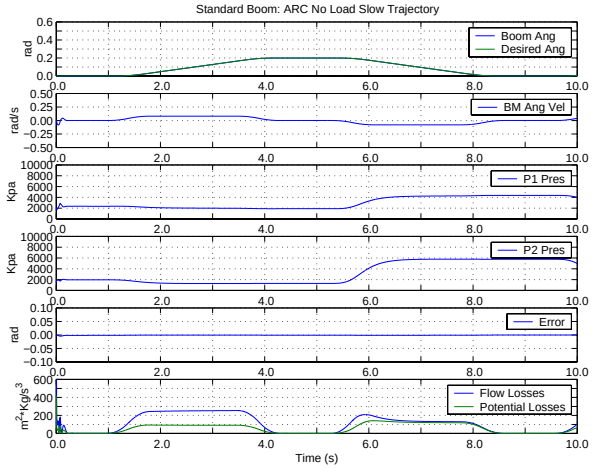

Figure 6. Standard Boom ARC Sim: Slow Traj. No Load

The simulation results show that the claims made about the use of a programmable valve with an adaptive robust controller and pressure regulator are substantiated. The good tracking performance is seen as well as significant gains in energy saving through sustaining the lowest possible chamber pressures.

The completed controller is also implemented on the hydraulic system and tested identically to the tests run in

the simulation results. In the actual implementation of the controller a number changes are necessary. Due to limited bandwidth of the valve the controller gains are lowered to prevent control chattering. The ARC gains as well as the gains for the pressure controller are changed. The ARC motion controller parameters used in the experiments are: $k_1 = k_2 = k_3 = 35$, Γ=*diag (1e-12, 1e-10, 5e4)*. The parameters for the pressure regulators are $k_{p1} = 1.3\times10^{-10}$, $\gamma_{Q1} = 2.8\times10^{-9}$ $k_{p2} = 1.8\times10^{-10}$, $\gamma_{Q2} = 3.15\times10^{-9}$.

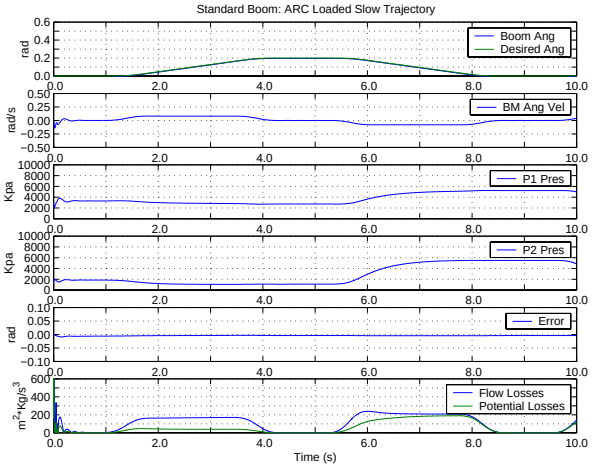

Figure 7. Standard Boom ARC Sim: Slow Traj. 50lb Load

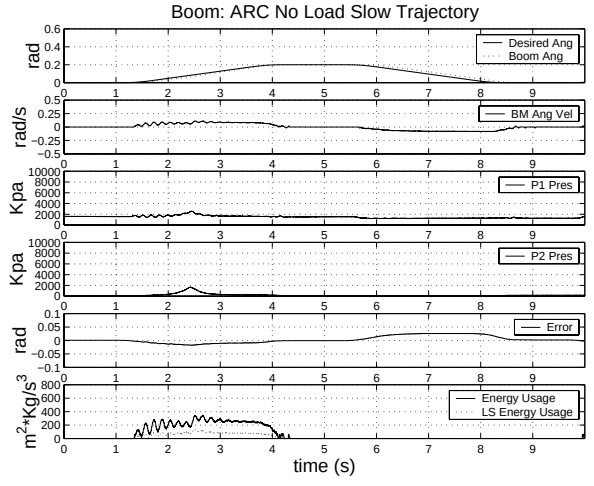

Figure 8. Boom ARC Exp: Slow Traj. No. Load

The experimental results for the slow point to point trajectory with and without a 50 lb. load, Fig. 8 and Fig. 9 show that the controller performs well in each case with a maximum error of 0.02 rad . The difference between the simulation and experimental results is the differing gains used. The cylinder pressures in both cases remain very low, thus reducing energy usage of the system. The energy usage is calculated as the pump flow times the pressure drop from pump to tank. The energy usage is zero when the cylinder is working in T3 mode when regeneration flow is used, as seen between the time of 5-9 seconds. The plot of the energy usage includes an additional line representing the potential decrease in energy usage with a load sensing pump as seen in the simulation results.

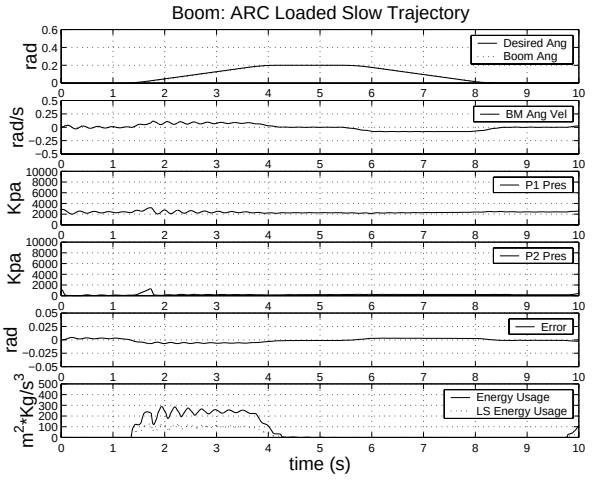

Figure 9. Boom ARC Exp: Slow Traj. 50lb Load

The experimental results show that the claims made about the use of a programmable valve with an adaptive robust controller and pressure controller are substantiated. The good tracking performance is seen as well as significant gains in energy saving through sustaining the lowest possible chamber pressures. The slight loss of performance seen in the experimental results is due to the limitation of the valve bandwidth.

CONCLUSION

The utilization of the programmable valve and the incorporation of a pressure controller and adaptive robust controller as detailed in this paper results in significant gains in reducing pump energy usage while achieving good tracking performance of an electro-hydraulic robot arm. The simulation and experimental results show that the significant gains in energy efficiency can be realized through the unique ability of the programmable valve to control both motion and chamber pressure as well as the ability of the valve to provide cost free regenerative flow.

ACKNOWLEDGMENTS

The project is supported in part by the National Science Foundation under the CAREER grant CMS-9734345. The fund from the Purdue Electro-Hydraulic Research Center supported by the Caterpillar Inc. and the donation of cartridge valves by Vickers Inc. for setting up the programmable valves used in the experiments is gracefully acknowledged.

REFERENCES

1. J.A.Aardema and D.W.Koehler. System and method for controlling an independent metering valve. *United Sates Patent*, (5,947,140), 1999
2. Ruth Book and Carrol E.Goeging, Programmable electrohydraulic valve. SAE, 01(2):28-34, 1999
3. F.Bu and Bin Yao. Adaptive robust precision motion control of single-rod hydraulic actuators with time-varying unknown inertia: a case study. In *ASME International Mechanical Engineering Congress and Exposition (IMECE), FPST-Vol.6*,131-138, 1999
4. F.Bu and Bin Yao. Nonlinear adaptive robust control of hydraulic actuators regulated by proportional directional control valves with deadband and nonlinear flow gain coefficients. In *Proc. of American Control Conference*, 4129-4133, 2000
5. K.D.Garnjost. Energy-conserving regenerative-flow valves for hydraulic servomoters. *United Sates Patent*, (4,840,111), 1989.
6. Arne Jansson and Jan-Ove Palmberg. Separate controls of meter-in and meter-out orifices in mobile hydraulic systems. *SAE Transactions*, 99)Sect 2): 377-383, 1990
7. K.D.Kramer and E.H.Fletcher. Electrohydraulic valve system. *United States Patent*, (Re.33,846), 1990
8. M.Krstic, I.Kanellakopoulos, and P.V.Kokotovic. *Nonlinear and adaptive control design*. Wiley, New York, 1995.
9. H.E.Merritt. *Hydraulic control systems*. Wiley, New York, 1967
10. Bin Yao. High performance adaptive robust control of nonlinear systems: a general framework and new schemes. In *Proc. of IEEE Conference on Decision and Control*, 2489-2494, 1997
11. Bin Yao and M. Tomizuka. Adaptive robust control of SISO nonlinear systems in a semi-strict feedback form. *Automatica*, 33(5):893-900, 1997.
12. Bin Yao and M. Tomizuka. Adaptive robust control of MIMO nonlinear systems in semi-strict feedback forms. *Automatica*, 2000.(Accepted) Parts of the paper were presented in the *IEEE Conf. On Decision and Control*, 2346-2351, 1995, and the *IFAC World Congress*, Vol. F, 335-340, 1996
13. B.Yao and M.Tomizuka. Smooth robust adaptive sliding mode control of robot manipulator with guaranteed transient performance. In *Proc. of American Control Conference*, 1176-1180, 1994. The full paper appeared in *ASME Journal of Dynamic Systems, Measurement and Control*, Vol. 118, No.4 764-775, 1996

CONTACT

Bin Yao.
1288 Mechanical Engineering Building
School of Mechanical Engineering
Purdue University
West Lafayette, IN 47907-1288
Phone: 765-494-7746
Fax: 765-494-0539
Email: byao@ecn.purdue.edu

APPENDIX A

Define a positive semi-definite function V_{ps} as

$$V_{ps} = \frac{1}{2}\theta_\beta e p_1^2 \tag{A1}$$

Differentiate (A1), while noting (19)

$$\begin{aligned}\dot{V}_{ps}(t) &= -\frac{k_p}{V_1} e p_1^2 + e p_1\left[\frac{1}{V_1}(Q_{1ms2} - \tilde{\theta}_Q + \Delta Q_1) + \dot{\theta}_\beta \dot{P}_{1d}\right] \\ &\le -\frac{2k_p}{\theta_\beta V_1} V_{ps} + \varepsilon_p \le -\lambda V_{ps} + \varepsilon_p\end{aligned} \tag{A2}$$

where $\lambda = \min(\frac{2k_p}{\theta_\beta V_1})$. This leads to

$$V_{ps}(t) \le \exp(-\lambda t) V_{ps}(0) + \frac{\varepsilon_p}{\lambda}[1 - \exp(-\lambda t)] \tag{A3}$$

which means a prescribed transient performance and bounded tracking error. When the uncertain disturbance $\Delta Q_1 = 0$, consider the augmented positive semi-definite function V_{pa} as

$$V_{pa} = V_{ps} + \frac{1}{2\gamma_\beta}\tilde{\theta}_\beta^2 + \frac{1}{2\gamma_Q V_1}\tilde{\theta}_Q^2 \tag{A4}$$

Differentiate (A4), while noting (A2) with $\Delta Q_1 = 0$,

$$\begin{aligned}\dot{V}_{pa} &= -\frac{k_p}{V_1} e p_1^2 + \frac{\tilde{\theta}_Q}{\gamma_Q V_1}(\dot{\hat{\theta}}_Q - \gamma_Q e p_1) \\ &+ \frac{\tilde{\theta}_\beta}{\gamma_\beta}(\dot{\hat{\theta}}_\beta + \gamma_\beta e p_1 \dot{P}_{1d}) + \frac{1}{V_1} e p_1 Q_{1Ms2}\end{aligned} \tag{A4}$$

It can be shown [13] that for any adaptation function τ, the projection mapping $\dot{\hat{\theta}} = \Pr oj_{\hat{\theta}}(\Gamma\tau)$ used in (22) guarantees

$$\begin{aligned}&\hat{\theta} \in \{\hat{\theta} : \theta_{\min} \le \hat{\theta} \le \theta_{\max}\} \\ &\tilde{\theta}^T(\Gamma^{-1}\Pr oj_{\hat{\theta}}(\Gamma\tau) - \tau) \le 0,\end{aligned} \tag{A5}$$

From (A4) and (A5), while noting (22),

$$\dot{V}_{pa} \le -\frac{k_p}{V_1}\varepsilon_p^2 \tag{A6}$$

Therefore, $ep_1 \in L_2$. It is also easy to check that $\dot{e}p_1$ is bounded. So, $ep_1 \to 0$ as $t \to \infty$ by Barbalat's lemma, which leads to the asymptotic tracking.

APPENDIX B

Define a positive semi-definite function V_2 as

$$V_2 = \frac{1}{2}\omega_2 z_2^2 \tag{B1}$$

Differentiate (B1), while noting (11) and (13)

$$\begin{aligned}\dot{V}_2 &= \frac{\theta_1}{J_c}\frac{\partial x_L}{\partial q_2}\omega_2 z_2 z_3 - \frac{\theta_1}{\theta_{1\min}}\omega_2 k_2 z_2^2 \\ &+\omega_2 z_2\left[\frac{\theta_1}{J_c}\frac{\partial x_L}{\partial q_2}P_{Lds2} - \tilde{\theta}^T\phi_2 + \tilde{T}\right]\end{aligned} \tag{B2}$$

Define a augmented positive semi-definite function V_3 as

$$V_3 = V_2 + \frac{1}{2}\omega_3 z_3^2 \tag{B3}$$

Differentiate (B3)

$$\begin{aligned}\dot{V}_3 &= -\frac{\theta_1}{\theta_{1\min}}\omega_2 k_2 z_2^2 - \frac{\theta_3}{\theta_{3\min}}\omega_3 k_3 z_3^2 \\ &+\omega_2 z_2\left[\frac{\theta_1}{J_c}\frac{\partial x_L}{\partial q_2}P_{Lds2} - \tilde{\theta}^T\phi_2 + \tilde{T}\right] \\ &+\omega_3 z_3\left[\theta_3 Q_{Lds2} - \tilde{\theta}^T\phi_3 + \theta_3\tilde{Q}_L - \frac{\partial P_{Ld}}{\partial\hat{\theta}}\dot{\hat{\theta}} + \tilde{T}\right] \\ &\le -\frac{\theta_1}{\theta_{1\min}}\omega_2 k_2 z_2^2 - \frac{\theta_3}{\theta_{3\min}}\omega_3 k_3 z_3^2 + \omega_2\varepsilon_2 + \omega_3\varepsilon_3 \\ &\le -\min\left(\frac{\theta_1}{\theta_{1\min}}k_2, \frac{\theta_3}{\theta_{3\min}}k_3\right)V_3 + (\omega_2\varepsilon_2 + \omega_3\varepsilon_3)\end{aligned} \tag{B4}$$

Similar to Appendix A, (B4) shows a prescribed tracking performance with bounded tracking error.

APPENDIX C

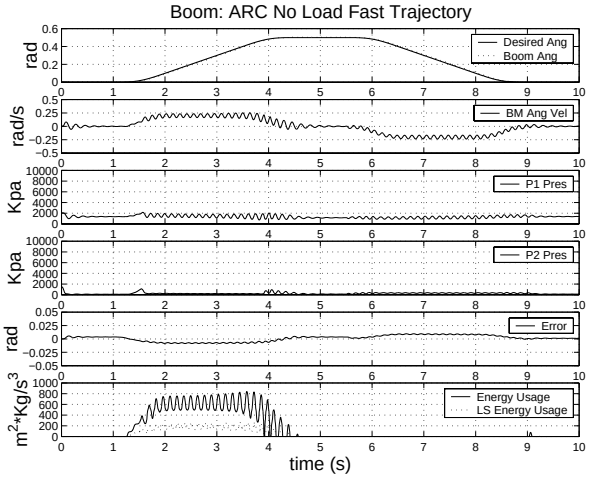

Figure 10. Boom ARC Sim: Fast Traj. No Load

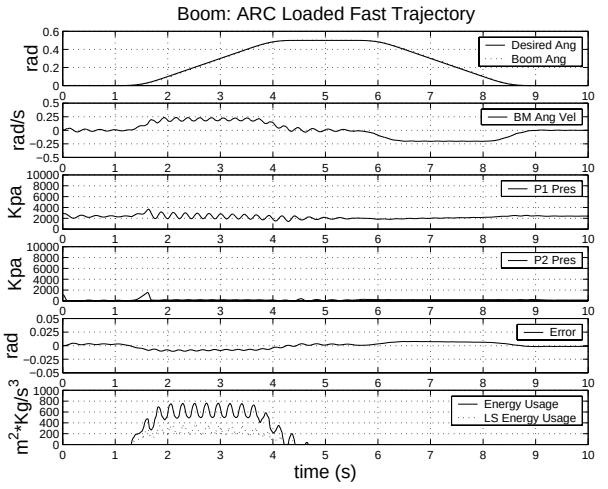

Figure 11. Boom ARC Sim: Fast Traj. 50 Load

APPENDIX D

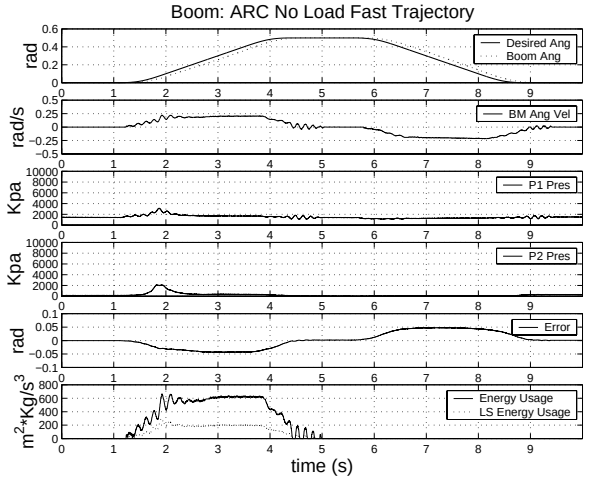

Figure 12 Boom ARC Exp: Fast Traj. No Load

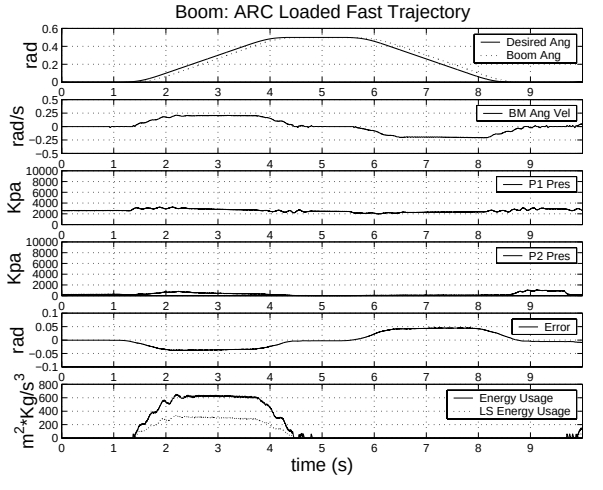

Figure 13. Boom ARC Exp: Fast Traj. 50lb Load